$(Gd,Yb,Tb)PO_4$ Up-Conversion Nanocrystals for Bimodal Luminescence-MR Imaging

Mengistie L. Debasu,[a,b] D. Ananias,[b] Sonia L. C. Pinho,[b] Carlos F.G.C. Geraldes,[c,d,e] Luís D. Carlos,[a],* João Rocha[b],*

[a]*Department of Physics*, [b]*Department of Chemistry, CICECO, University of Aveiro, 3810-193 Aveiro, Portugal*

[c]*Department of Life Sciences, Faculty of Science and Technology, University of Coimbra, P.O. Box, 3001-401 Coimbra, Portugal.*

[d]*Center of Neurosciences and Cell Biology, University of Coimbra, Largo Marquês de Pombal, 3004-517 Coimbra, Portugal*

[e]*Centro de Química de Coimbra, Rua Larga, University of Coimbra, 3004-535 Coimbra, Portugal*

**E-mail: lcarlos@ua.pt, rocha@ua.pt*

Supplementary Information

1. Synthesis

Up-conversion monoclinic $(Gd,Yb,Tb)PO_4$ nanocrystals were synthesized by a hydrothermal route at 150 ºC as described schematically in Fig.S1.

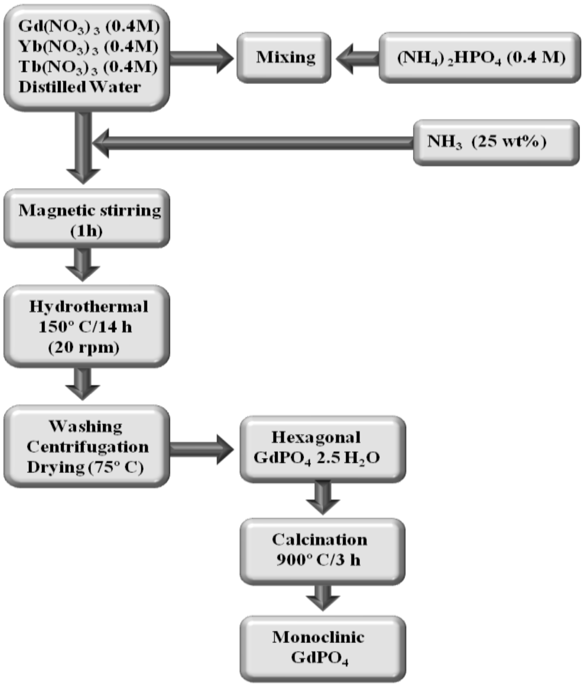

Fig.S1 A schematic representation for the synthesis of up-conversion monoclinic (Gd,Yb,Tb)PO4 nanocrystals.

2. XRD patterns

The powder X-ray diffraction (XRD) patterns of (Gd,Yb,Tb)PO_4 nanocrystals/microcrystals, as-synthesized and after calcination, are shown in Fig.S2A. The as-synthesized sample gave broad diffraction peaks, indexed into the hexagonal samarium phosphate hydrate ($SmPO_4\cdot2.5H_2O$), with space group P6222 (PDF-00-027-0583). It is therefore concluded that the hydrated hexagonal (Gd,Yb,Tb)$PO_4\cdot2.5H_2O$ phase formed prior to calcination. This phase remains unchanged after heat treatment up to 500 ^oC for 3 hours. Heating the samples at 700, 900 and 1200 ^oC for 3 hours results in a monazite-type monoclinic $GdPO_4$ phase having space group P21/n (PDF-01-083-0657) (Fig.S2A). Relatively sharp diffraction peaks were obtained at high calcination temperature (Fig.S2B), indicating that increasing the calcination temperature significantly increases the crystal size (5 nm for as-synthesized sample and 140 nm for the sample obtained after calcination at 1200 ºC).

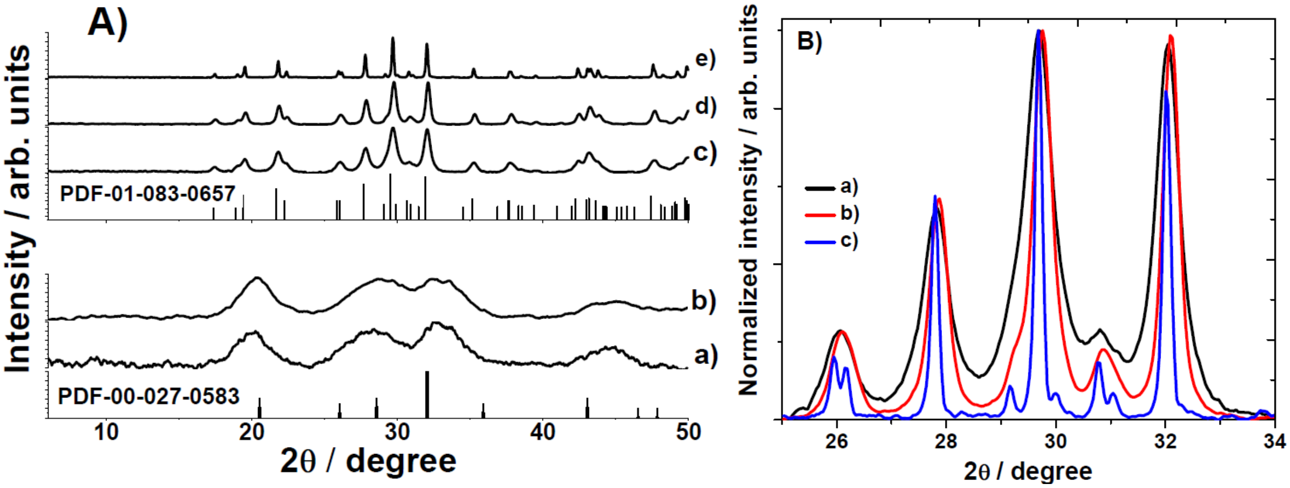

Fig.S2 A) XRD patterns of a) and b) as-synthesized $Gd_{0.87}Yb_{0.10}Tb_{0.03}PO_4\cdot2.5H_2O$ nanocrystals (hexagonal phase) and after calcination at 500 ^oC/3h, respectively, monoclinic $Gd_{0.87}Yb_{0.10}Tb_{0.03}PO_4$ after calcination at c) 700 ºC/3h, d) 900 ºC/3h and e) 1200 ºC/3h; B) shows the effect of the calcination temperature on the broadening of the diffraction peaks for monoclinic $Gd_{0.87}Yb_{0.10}Tb_{0.03}PO_4$ obtained after heat treatment of the parent hexagonal phase at a) 700 ºC/3h, b) 900 ºC/3h and c) 1200 ºC/3h.

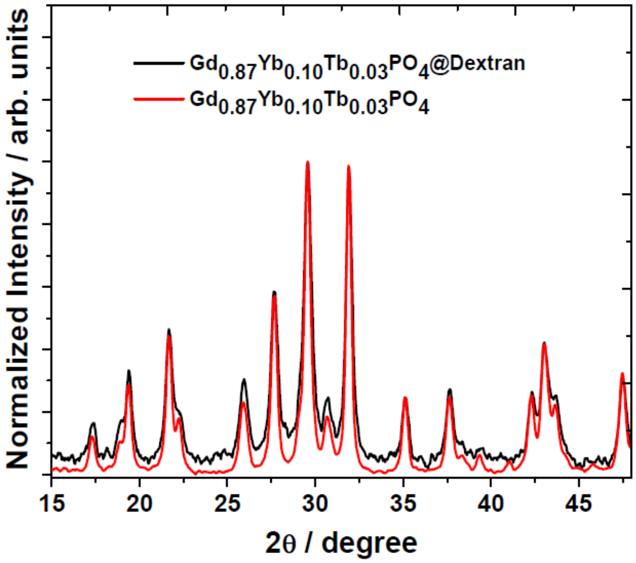

Fig.S3 XRD patterns for dextran-coated (black line) and uncoated (red line) monoclinic $Gd_{0.87}Yb_{0.10}Tb_{0.03}PO_4$.

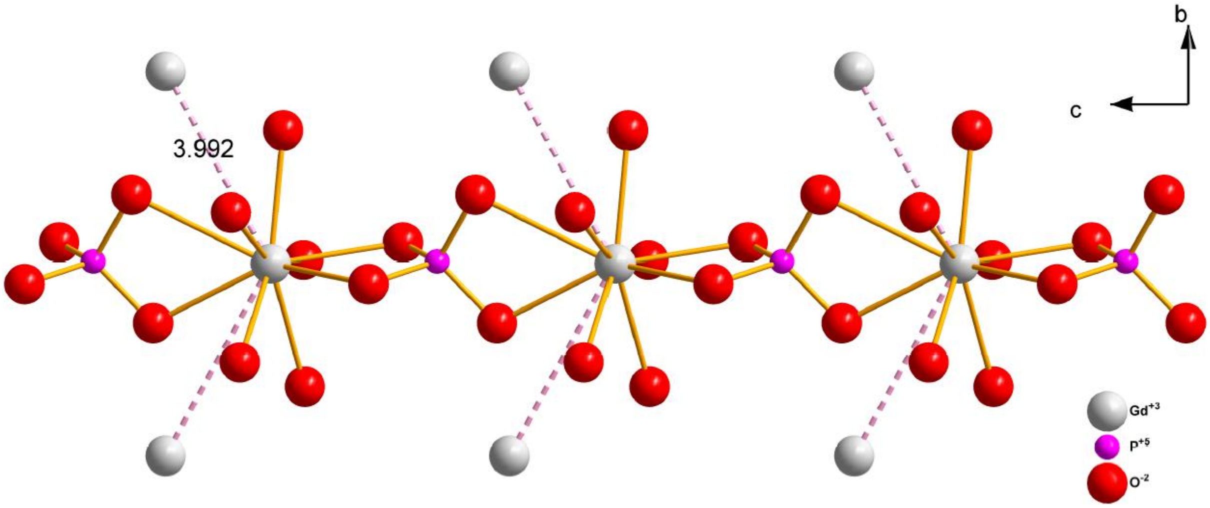

Fig. S4 Atomic arrangement of monoclinic $GdPO_4$ viewing along the [-100] direction and the nearest-neighbor Gd^{3+}-Gd^{3+} distance (broken lines), 3.992 Å.

3. TEM images

TEM images of as-synthesized nanocrystals and after heat treatment of the as-synthesized one at different temperatures are shown in Fig.S5. The samples before calcinations are in fact much smaller in size and an attempt to collect high resolution TEM images for this sample was not successful as the sample was not stable and undergoing phase transformation during imaging. The shape of the nanocrystals is irregular, not well-defined. However, it can be seen that increasing the calcination temperature significantly increases the particle size (Fig.S5-6), which is also evidenced with the XRD patterns shown in Fig.S2.

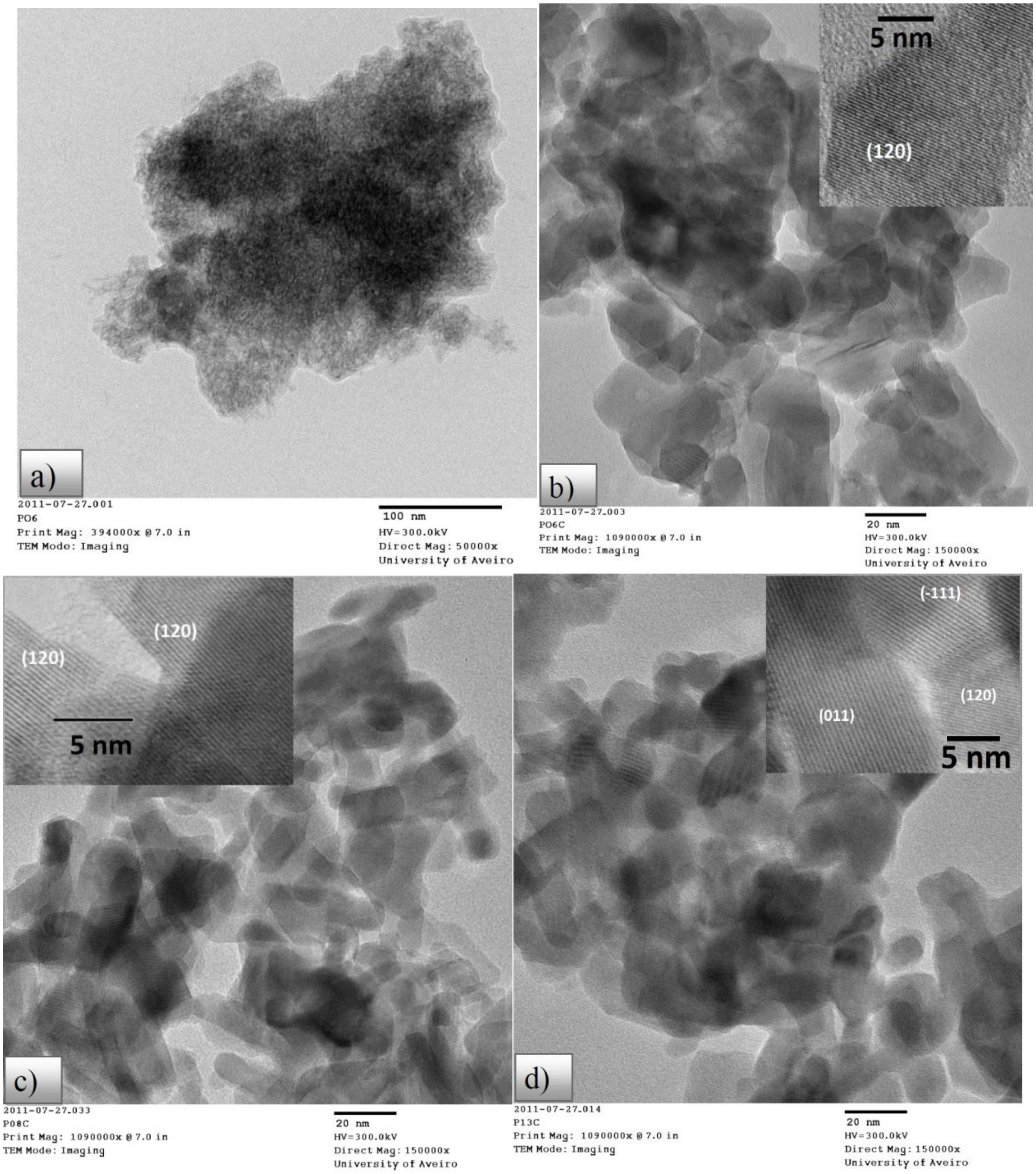

Fig.S5 TEM images of a) hexagonal $Gd_{0.85}Yb_{0.10}Tb_{0.05}PO_4 \cdot 2.5H_2O$ nanocrystals before calcination, monoclinic b) $Gd_{0.85}Yb_{0.10}Tb_{0.05}PO_4$, c) $Gd_{0.87}Yb_{0.10}Tb_{0.03}PO_4$ and d) $Gd_{0.85}Yb_{0.10}Tb_{0.01}PO_4$ nanocrystals obtained after calcination at 900 ºC for 3 hours.

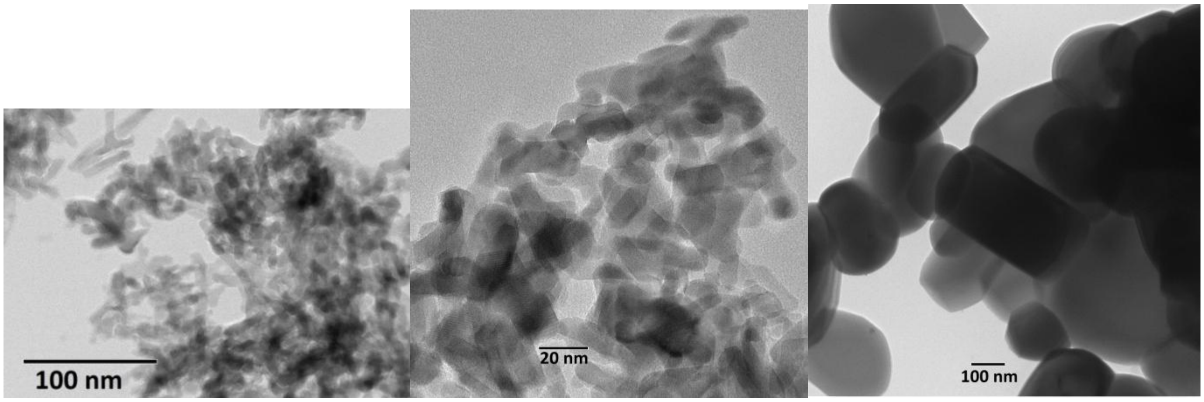

Fig. S6 TEM images of monoclinic $Gd_{0.87}Yb_{0.10}Tb_{0.03}PO_4$ nanocrystals/microcrystals calcined at 700, 900 and 1200 ºC for 3 hours (from left to right, respectively), showing that crystal size increases on increasing the calcination temperature.

4. FT-IR Spectra

The infrared spectra of the nanocrystals are shown in Fig.S7. The broad band around 3454 cm^{-1} is attributed to the water -OH stretching vibration while the band centered at 1640 cm^{-1} is the corresponding bending vibration.[1-2] However, the appearance of these peaks at 3454 and 1640 cm^{-1} with relatively weak intensities after calcination at 900 ºC should be due to the moisture in air physically adsorbed on the surface of the nanoparticles during the measurements or storage period of the samples. The peaks at 1076, 624 and 536 cm^{-1} correspond to P-O stretching, O=P-O bending, and O-P-O bending modes, respectively.[2-3] For the calcined samples, an additional peak around 574 cm^{-1} ascribed to the O-P-O stretching mode [1,3] was detected, indicating the presence of phase transformation.[4]

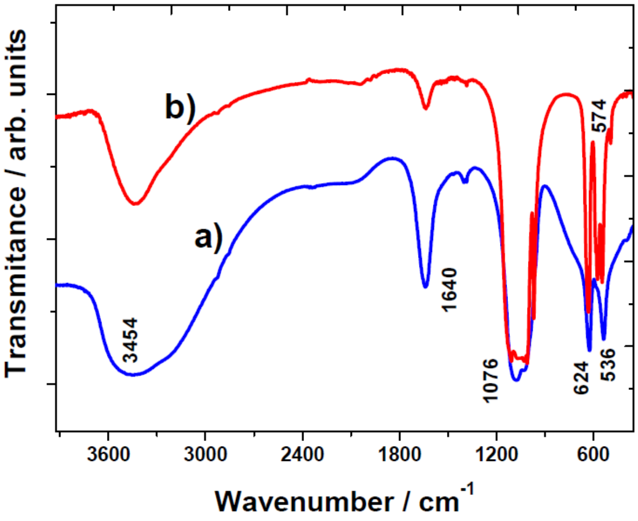

Fig.S7 FT-IR spectra a) as-synthesized $Gd_{0.87}Yb_{0.10}Tb_{0.03}PO_4 \cdot 2.5H_2O$ nanocrystals and b) monoclinic $Gd_{0.87}Yb_{0.10}Tb_{0.03}PO_4$ nanocrystals obtained after calcination at 900 ºC for 3 hours.

5. Up-conversion emissions

Fig.S8 shows the pump-power dependence of up-conversion emission spectra for the monoclinic (Gd,Yb,Tb)PO_4 nanocrystals upon a 980 nm CW laser diode excitation. It should be noted that the intensity of the up-conversion emission strongly depends on the pump-power.

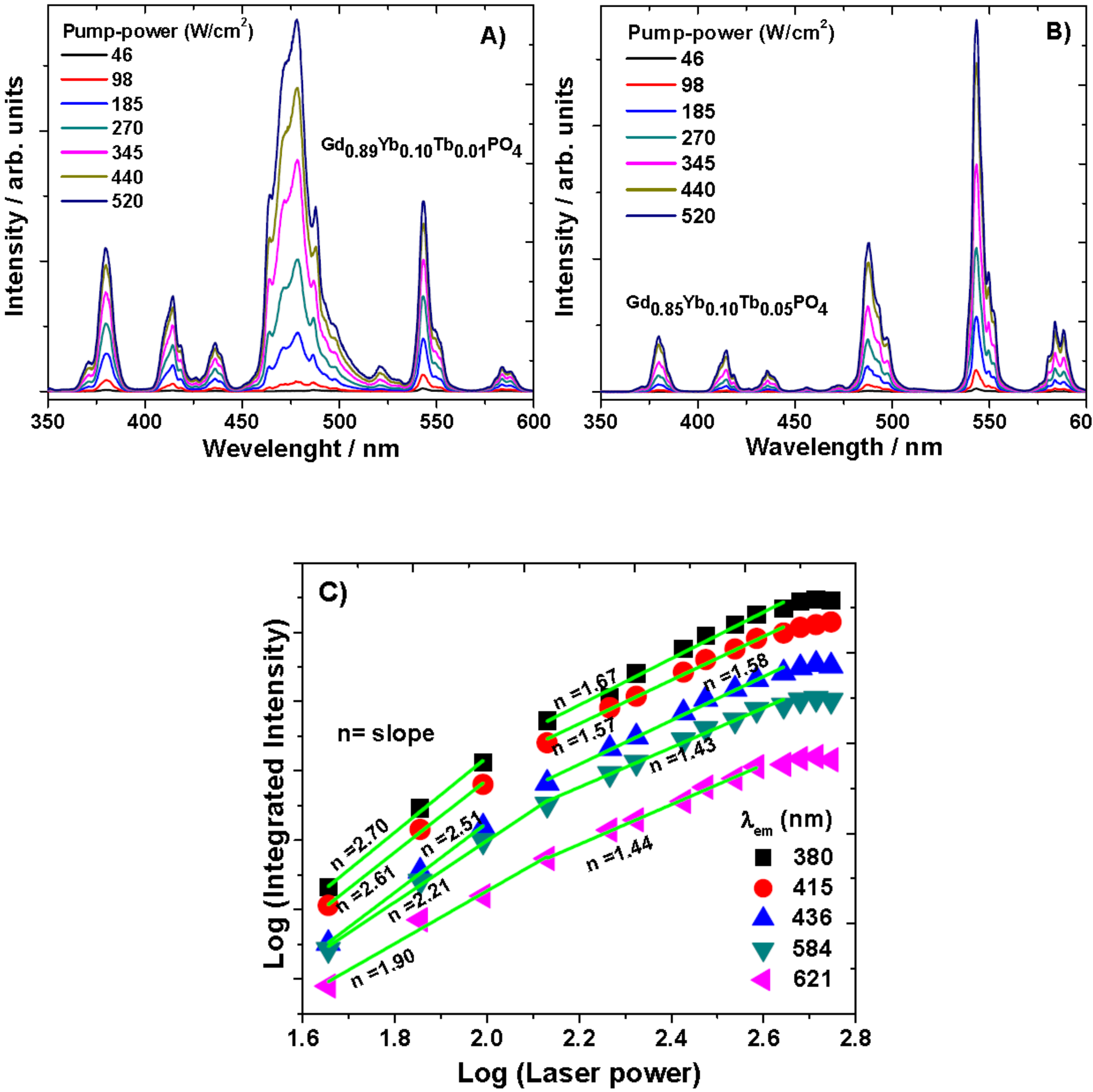

Fig.S8 Pump-power (W/cm^2) dependence of the up-conversion emission intensities for A) $Gd_{0.89}Yb_{0.10}Tb_{0.01}PO_{4,}$ B) $Gd_{0.85}Yb_{0.10}Tb_{0.05}PO_4$ nanocrystals obtained after calcination at 900 ^oC for 3 hours and C) double-log plots of pump-power vs integrated emission intensity of the bands at 380, 415, 436, 584 and 621 nm for $Gd_{0.89}Yb_{0.10}Tb_{0.01}PO_4$.

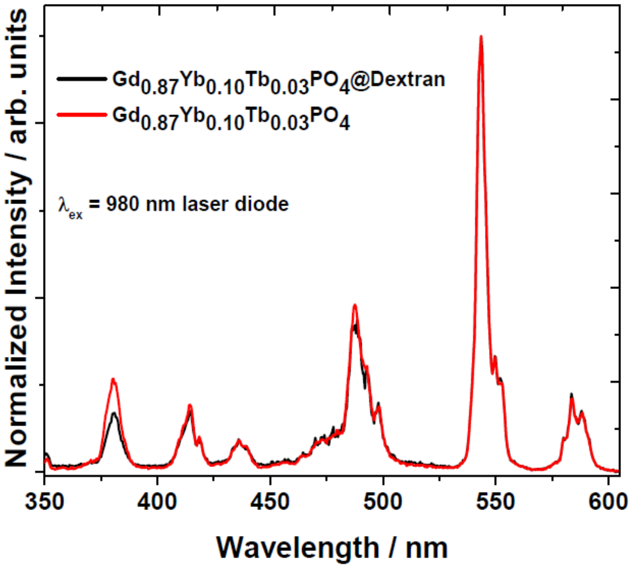

Fig.S9 Comparison of the up-conversion emission for dextran-coated and uncoated monoclinic $Gd_{0.87}Yb_{0.10}Tb_{0.03}PO_4$ nanocrystals under excitation at 60 mW with a 980 nm laser diode.

6. Effect of calcination temperature (particle size) on up-conversion emissions

It was noted that raising the calcination temperature above 900 ^{o}C significantly enhances the up-conversion emission intensities of all samples (visible to the naked eye even at relatively low pump-power). This is mainly due to the changing particle size because at low calcination temperature the nanoparticles are smaller, having a relatively high surface-to-volume ratio, with most emitting ions on the surface subjected to non-radiative mechanisms. Consequently, no up-conversion emission was observed for the samples calcined at 300, 500 and 700 ^{o}C for 3 hours. A strong blue cooperative up-conversion emission of Yb^{3+} was observed after the samples were calcined at 900 ^{o}C and for 10.0-30.0 mol% Yb^{3+}/0.5-1.0 mol% Tb^{3+}. Therefore it should be noted that the cooperative emission is strongly dependent on the calcination temperature and concentration of Yb^{3+} and Tb^{3+}. As shown in Fig.S10, additional transition lines that could be attributed to the cooperative emission of coupled Yb^{3+}/Yb^{3+} appeared for the sample calcined at 1200 ºC, in contrast to those calcined at 900 ºC. This may be explained by the changing particle size due to the calcination temperature. Because at high calcination temperature the particle size was increased (Fig.S2) which in turn may decrease the non-radiative channels that are strong in the smaller particles. Moreover, increasing the particle size may modify the Yb^{3+}-Yb^{3+} pair interaction and thus create favorable conditions to form a pair of excited Yb^{3+} ions active for the cooperative emission.[5-6] The cooperative emissions are thus more likely to be efficient in bigger particles.

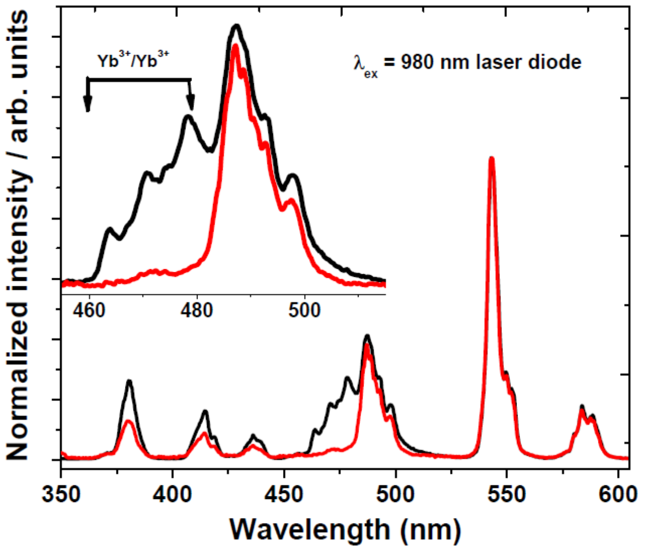

Fig.S10 Dependence of up-conversion emission spectra of monoclinic $Gd_{0.85}Yb_{0.10}Tb_{0.05}PO_4$ nanocrystals on the calcination temperature at 900 °C/3h (red line) and at 1200 °C/3h (black line).

7. Relaxivity Measurements

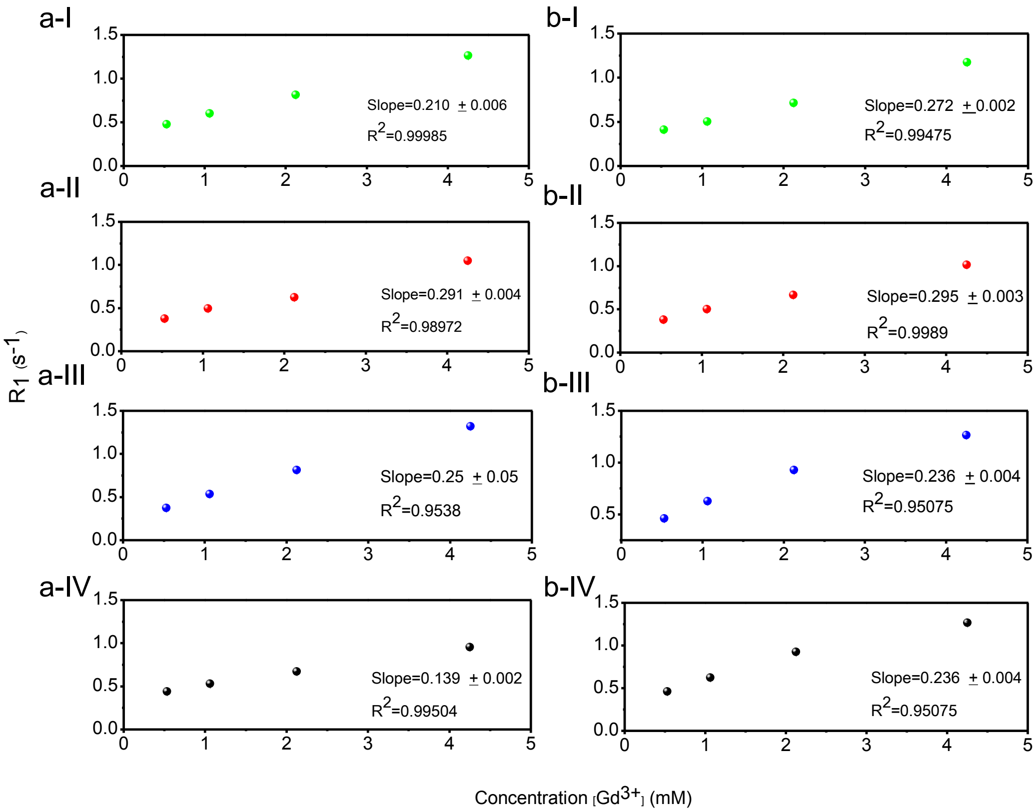

Fig.S11 Proton relaxation rates R_1 vs. Gd(III) concentration measured at 20 MHz (a) 25 ºC and (b) 37 ºC for aqueous solutions of samples: I- $GdPO_4$; II- $Gd_{0.85}Yb_{0.10}Tb_{0.05}PO_4$; III- $Gd_{0.87}Yb_{0.10}Tb_{0.03}PO_4$ and IV- $Gd_{0.87}Yb_{0.10}Tb_{0.03}PO_4$@Dextran.

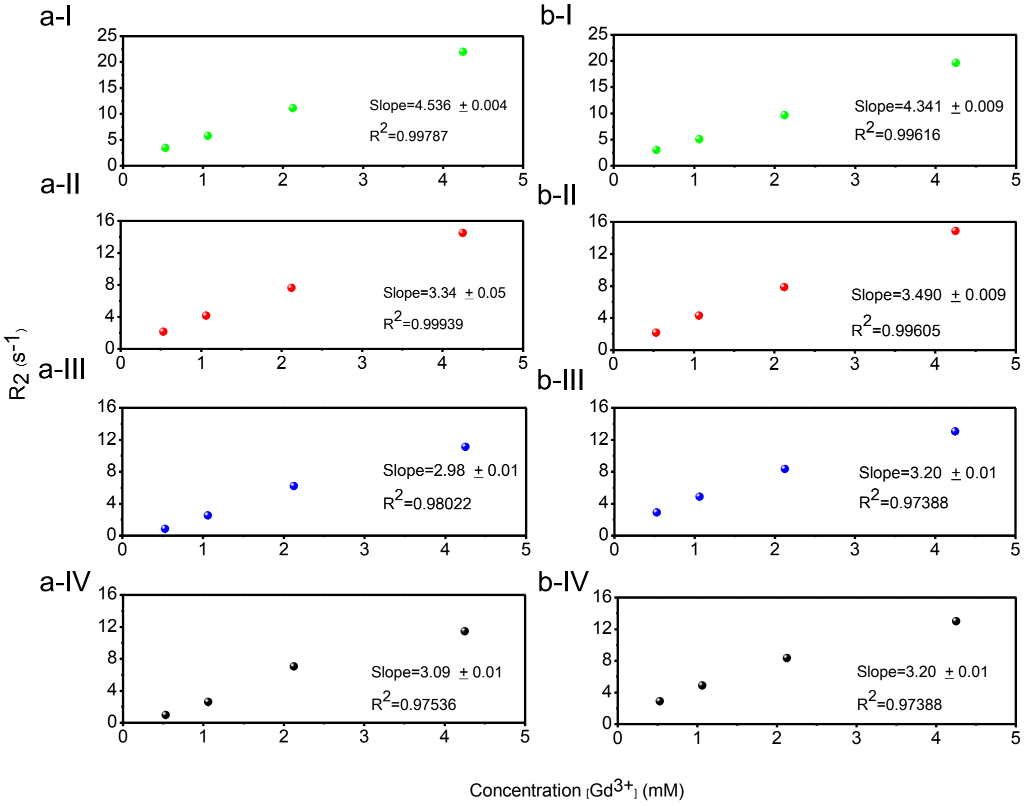

Fig.S12 Proton relaxation rates R_1 vs. Gd(III) concentration measured at 20 MHz (a) 25 ºC and (b) 37 ºC for aqueous solutions of samples: I- $GdPO_4$; II- $Gd_{0.85}Yb_{0.10}Tb_{0.05}PO_4$; III- $Gd_{0.87}Yb_{0.10}Tb_{0.03}PO_4$ and IV- $Gd_{0.87}Yb_{0.10}Tb_{0.03}PO_4$@Dextran.

8. Leaching Test

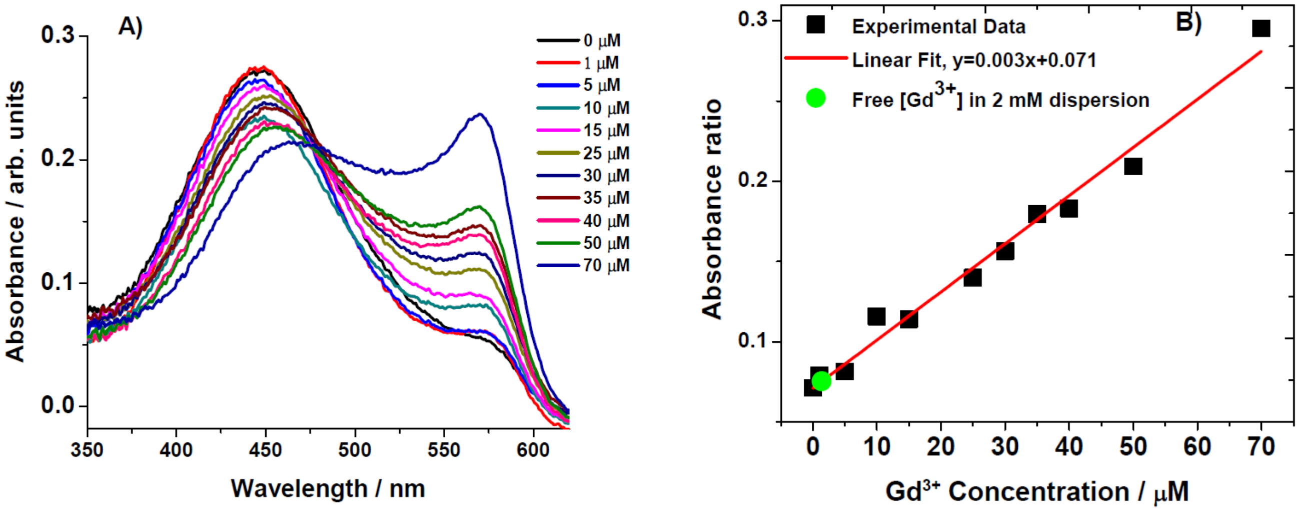

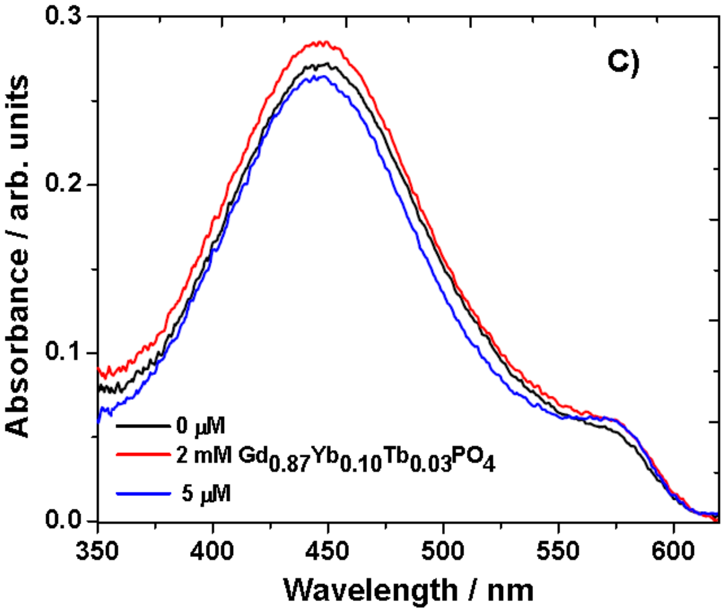

Fig.S13 A) UV-visible absorption spectra of xylenol orange solution (18 µM) containing different concentrations of Gd^{3+}, B) the corresponding calibration curve (black squares) and the amount of free Gd^{3+} in 2 mM of aqueous dispersion of $Gd_{0.87}Yb_{0.10}Tb_{0.03}PO_4$ stored at 4 ºC for a week (1.41 µM, green circle) and C) comparison of UV-visible absorption spectra of xylenol orange solution (18 µM) with 0 µM Gd^{3+} (black line), with 5 µM Gd^{3+} (blue line) and with 2 mM aqueous dispersion of $Gd_{0.87}Yb_{0.10}Tb_{0.03}PO_4$ (red line), showing that there is insignificant change on the intensity of the absorption band at 573 nm with the presence of nanoparticles (*i.e.*, Gd^{3+} leaching is negligible).

9. Steady-state excitation/emission

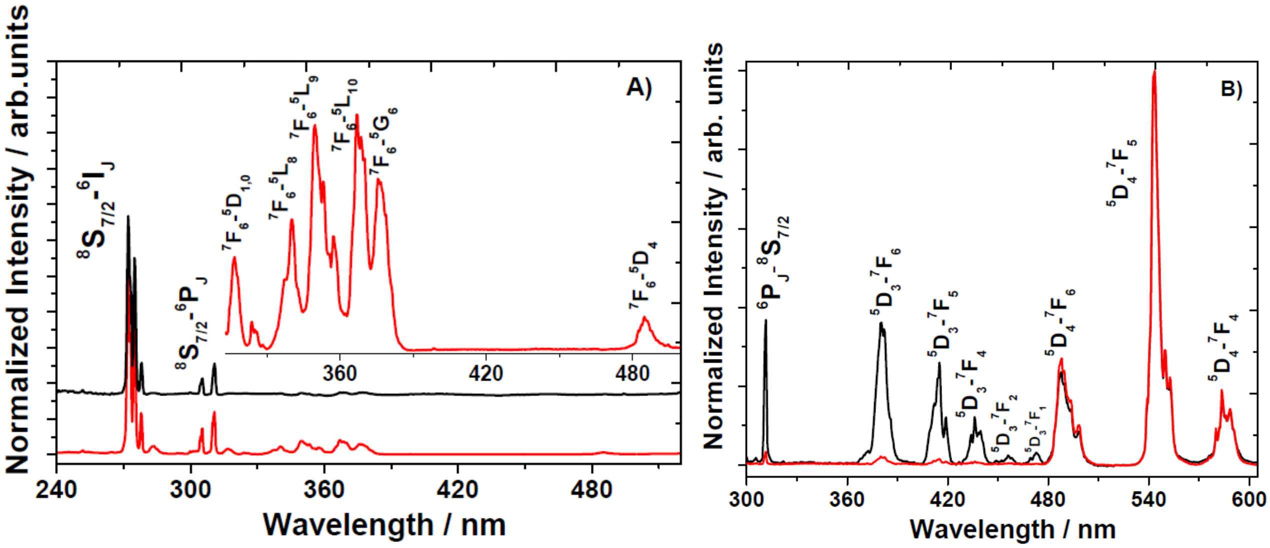

Fig.S14 Steady-state A) excitation spectra monitoring the emission at 543 nm, and B) emission spectra using the excitation at 272 nm of $Gd_{0.895}Yb_{0.10}Tb_{0.005}PO_4$ (black line) and $Gd_{0.85}Yb_{0.10}Tb_{0.05}PO_4$ (red line) nanocrystals. The inset in A shows the intra-4f-4f transitions of Tb^{3+}. Note that, unlike the up-conversion emission band at 479 nm, the down-conversion emission shows only the Gd^{3+} and Tb^{3+} emissions.

References:

1 R. Kijkowska, E. Cholewka and B. Dusza, *J. Mater. Sci.* 2003, **38**, 223.
2 H. Wang, G. Li, X. Guan and L. Li, *J. Alloys Compd.* 2011, **509**, 4160.
3 P.C. de Sousa Filho and O.A. Serra, *J. Phys. Chem. C* 2011, **115**, 636.
4 R. Kijkowska, *Thermochim. Acta* 2003, **404**, 81.
5 J. Amami, D. Hreniak, Y. Guyot, R. Pazik, C. Goutaudier, G. Boulon and M. Ayadi, W. Strek, *J. Lumin.* 2006, **119-120**, 383.
6 G. Boulon and V. Lupei, *J. Lumin.* 2007, **125**, 45.